Desalination and Water Treatment
www.deswater.com

doi: 10/5004/dwt.2012.3105

Taylor & Francis
Taylor & Francis Group

44 (2012) 245–254
June

Modeling of equilibrium and kinetics of chlorobenzene (CB) adsorption onto powdered activated carbon (PAC) for drinking water treatment

Ming-li Lin[a], Zhi-wei Zhao[a,*], Fu-yi Cui[a], Sherngji Xia[b]

[a]*State Key Laboratory of Urban Water Resource and Environment, School of Municipal and Environmental Engineering, Harbin Institute of Technology, No. 73 Huanghe Road, Nangang District, Harbin 150090, P.R. China*
Tel. +86 13466794876; Fax: +86 10 58934694; email: hhdxlml@163.com
[b]*State Key laboratory of Pollution Control and Resources Reuse, Tongji University, Shanghai, 200092, China*

Received 13 July 2011; Accepted 7 November 2011

ABSTRACT

A batch system was applied to study the adsorption equilibrium and kinetics of chlorobenzene (CB) from aqueous solution by powdered activated carbon (PAC). Adsorption isotherm was determined at 25°C and the experimental data obtained were mathematically modeled with the Langmuir, Freundlich, Langmuir–Freundlich and Toth equations. Non-linear regression and Chi-square (χ^2) analysis have been undertaken to determine the best isotherm and isotherm parameters. The Langmuir–Freundlich model yielded the best fit to the experimental data. The influence of two experimental parameters, initial CB concentration and PAC dose, on the adsorption kinetics was evaluated. The kinetics data obtained were modeled by pseudo-first-order, pseudo-second-order, and Langmuir–Freundlich kinetic models, respectively. The rate constants of Langmuir–Freundlich kinetic model obtained by extended geometric method are independent of initial CB concentration and PAC dose. The results show that the adsorption amount and relative removal of CB at any time for any initial CB concentration and any PAC dose can be estimated directly with the rate constants by using the Langmuir–Freundlich kinetic model.

Keywords: Chlorobenzene; Equilibrium isotherm; Kinetics; Adsorption; Powdered activated carbon (PAC); Water treatment

1. Introduction

Halogenated aromatic compounds are important environmental pollutants in surface water. CB is among these compounds due to its widespread applications, such as paint removing formation, heat transfer media, engine cleaners, toilet block deodorants, dyestuffs, pesticide, and pharmaceutical intermediates and mothproofing agents [1,2]. The improper disposal together with the slow degradation and unpleasant taste and odor [3] led to its ubiquity in water environment and to the necessity of finding effective remediation technologies for its removal. This is particularly true when surface water is utilized as drinking water for CB in surface water has a potential risk to human health. The Chinese drinking water quality standards set the maximum allowable concentration of CB at 0.3 mg l^{-1} (2.67×10^{-6} M). Some water treatment processes have been developed and put into practice to meet this limit.

As one of volatile organic compounds (VOCs), CB in water can be generally treated with air stripping and powdered activated carbon (PAC) adsorption.

*Corresponding author.

Air stripping yields 95–99% removal of VOCs [4]. However, because of environmental issues, discharge of CB into the atmosphere limits its use. On the other hand, PAC adsorption processes in drinking water treatment can effectively control problems related to trace organic substances such as taste- and odor-causing compounds, VOCs, and synthetic organic compounds (SOC) including pesticides. As a result, the use of PAC in drinking water treatment has gained popularity because (1) PAC can be applied only when it is needed, for example, during a pollution episode such as elevated pesticide concentrations during summer runoff or a chemical spill in a river; (2) PAC can be fed in many drinking water treatment plants following a relatively small capital investment [5]. At the same time, the understanding of both adsorption equilibrium and kinetics is essential for proper design of operating conditions and analysis of economy. However, little information exists about CB adsorption equilibrium and kinetics onto PAC in aqueous, and only a few studies have quantified CB uptake and kinetics on alternative adsorbents such as marine sediments [1], activated montmorillonite [6], and cetyltrimethylammonium bromide (CTMAB) modified bentonite and kaolinite [7].

In this paper, we describe the adsorption equilibrium and kinetics of CB from buffered distilled-deionized water (DDW) onto PAC at several initial CB concentrations corresponding to minimum equilibrium concentration values of less than 0.3 mg l^{-1}, which is compatible with drinking water tolerance limits. Equilibrium adsorption isotherm was measured for single component system and the experimental data were analyzed by four commonly used models, namely the Langmuir, Freundlich, Langmuir–Freundlich, and Toth isotherm equations. Nonlinear regression analysis coupled with a detailed error analysis was undertaken to determine single component isotherm parameters and thus obtained the best-fit isotherm model and isotherm parameters. Kinetics experiments were also carried out to investigate the apparent adsorption rate (the net ratio of adsorption capacity to time, dq/dt, expressed as the difference between adsorption and desorption rates) of CB onto PAC at three different initial CB concentrations and three different PAC doses, respectively. The results were interpreted by pseudo-first-order, pseudo-second-order, and Langmuir–Freundlich kinetic models to determine the values of the rate constants and other kinetic parameters by assessing their dependence on the initial concentration or PAC dose. The determined equilibrium constants and kinetic constants should be ultimately useful for studies on adsorption in raw water and for defining the essential needs to better design adsorption process.

2. Materials and methods

2.1. Materials

Experiments were conducted in DDW with dissolved organic carbon (DOC) concentration of less than 0.2 mg l^{-1}. DDW water was adjusted to pH 7.2 with 1 mM phosphate buffer (0.5×10^{-3} M $Na_2HPO_4 \cdot H_2O$ and 0.5×10^{-3} M NaH_2PO_4).

Chlorobenzene (CB), a common drinking water contaminant, was used as the target contaminant. A stock solution was prepared by dissolving 100 mg l^{-1} of CB in ultrapure water without the use of non-aqueous solvents. The stock solution was stored at 4°C in a dark place for preparing all working solutions.

Commercial wood-based PAC HN-200 (supplied by Xianke Co.) was used in this study. This PAC had a geometric mean diameter of about 6 µm (determined using a Liquid Particle Counting system, HIAC 9703) and is commonly used for VOCs removal in drinking water treatment. The textural characteristics measured by nitrogen adsorption method at 77 K (ASAP 2020, Micrometritics, USA) are summarized in Table 1. Elements content (w/w) are C = 88.29%, O = 7.09%, H = 0.51%, and N = 0.91% (determined by an elemental analyzer,

Table 1
Textural characteristics of PAC

S_{BET}[a] (m^2g^{-1})	$S_{external}$[b] ($m^2 g^{-1}$)	S_{mic}[c] ($m^2 g^{-1}$)	Total pore volume[d] ($cm^3 g^{-1}$)	Micropore volume[e] ($cm^3 g^{-1}$)	Mesopore volume[f] ($cm^3 g^{-1}$)	Average pore diameter[g] (nm)
1210.212	775.803	434.409	0.692	0.190	0.394	2.69

[a]BET surface area.
[b]*t*-Plot external surface area.
[c]*t*-Plot micropore area.
[d]Single point adsorption total pore volume of pores less than 751.885 Å width at p/p° = 0.974.
[e]*t*-Plot micropore volume, pore size less than 20 Å.
[f]BJH Adsorption cumulative volume of pores between 17.000 Å and 3000.000 Å width.
[g]BJH Adsorption average pore width (4 V/A).

vario EL cube, Elementar). The PAC was randomly taken from a bulk bag, dried at 105°C overnight, then cooled and stored in an air-tight desiccators prior to use.

2.2. Methods

2.2.1. Equilibrium isotherm studies

The bottle point isotherm technique [8] was employed to determine the equilibrium capacity of PAC for CB. In an isotherm experiment, different amounts of carbon were added to glass bottles. Subsequently, a known volume of solution containing the target compound was transferred to the isotherm bottles (with no headspace), which were sealed using gastight rubber stoppers coated with a Teflon layer. Glass beads were added to each isotherm bottle to ensure proper mixing. The isotherm bottles were kept in a temperature-controlled shaking water bath with the jolting rate of 220 r min^{-1} at 25 ± 0.3°C for 24 h. Screening studies conducted over a 72 h period showed that equilibrium was reached within 24 h of agitation. Upon equilibration, adsorbents were separated from the liquid by filtration through 0.45 µm membrane filters. CB in the filtrate was analyzed by purge and trap GC-MS. The solid-phase concentration on the PAC was calculated via a mass balance. Three blanks were included with each isotherm experiment to evaluate adsorbate losses by mechanisms other than adsorption. The concentration of CB remained nearly constant (less than 2% of difference) in blanks over the 24 h equilibration time, revealing that the volatility of CB and its interaction with the bottles can be neglected.

2.2.2. Adsorption kinetic studies

Batch kinetic tests were conducted at 25 ± 0.3°C with the stirring rate of 220 r min^{-1} to determine the kinetic parameters that describe the rate of removal of CB by PAC. PAC used in the kinetic experiments was soaked overnight in ultrapure water to allow for complete wetting of the pores. Prior to the addition of PAC to a flask containing 1.4 l of working solution, samples were collected to determine the initial CB concentration. As the temperature of the solution reached 25°C, predetermined amount of PAC was added. Samples were taken at selected time intervals and filtered immediately for the analysis of liquid-phase CB concentration. The kinetics data were taken for 3 h.

2.2.3. Analysis

CB was extracted with an automatic Purge and Trap Sample Concentrator 4551A system (O.I. Analytical TX, USA) on-line coupled with the GC-MS system and equipped with a Tenax 4660 adsorbent trap (O.I. Analytical).

The samples placed in the vial were purged under the following conditions: 25 ml purge vessel (VOCARB 4000 Trap) and 40 ml min^{-1} ultra pure helium purge flow, purge-ready temperature: 30°C, purge time: 11 min, desorb time: 4 min, desorb temperature: 180°C, bake time: 10 min, bake temperature: 230°C.

The following GC–MS (thermo, Trace-DSQ) condition was used for the analysis of all water samples: ultra pure helium flow: 1.2 ml min^{-1}, split ratio: 20:1, injector temperature: 180°C, column (DB-5 ms, 30 m × 0.25 µm × 0.25 mm): 50°C hold 5 min, MS condition- ionization mode: electron ionization (EI), interface temperature: 220°C, ion source temperature: 200°C, detector scan (3 scan s^{-1}) mode: 35–300 amu, electronic ionization: 70 eV.

3. Results and discussion

3.1. Equilibrium isotherm

Adsorption properties and equilibrium data, commonly known as adsorption isotherms, describe how adsorbate molecules interact with adsorbent materials, and so are critical in optimizing the use of adsorbent. It is important to establish the most appropriate correlation for the equilibrium curve to optimize the design of an adsorption system to remove contaminant from solutions. Several adsorption equilibrium theories available in the literature such as Langmuir, Freundlich, Langmuir–Freundlich, and Toth isotherm models can be used to describe equilibrium studies. The mathematical equations of the four models are illustrated in Table 2.

Experimental data were compared by using the four isotherm models and the best-fitted model was determined based on the use of five error functions and Chi-square (Table 3) to calculate the error deviation between experimental and predicted equilibrium adsorption data [9,10]. Since the minimization of each of the error functions renders corresponding set of isotherm parameters, "sum of the normalized errors" (SNE) were used

Table 2
Mathematical equation of the used isotherm models

Isotherm models	Equations	
Langmuir	$q_e = q_{mL} \frac{K_L C_e}{1 + K_L C_e}$	(1)
Freundlich	$q_e = K_F C_e^{1/n_F}$	(2)
Langmuir–Freundlich	$q_e = q_{mLF} \frac{(K_{LF} C_e)^{m_{LF}}}{1 + (K_{LF} C_e)^{m_{LF}}}$	(3)
Toth	$q_e = q_{mT} \frac{K_T C_e}{(1 + (K_T C_e)^{n_T})^{1/n_T}}$	(4)

Table 3
Error functions and Chi-square

Error functions	Equations	
Sum of the squares of the errors (SSE)	$\mathrm{SSE} = \sum_{i=1}^{n} (q_{\mathrm{e,cal}} - q_{\mathrm{e,exp}})_i^2$	(5)
Sum of absolute errors (SAE)	$\mathrm{SAE} = \sum_{i=1}^{n} \left\lvert q_{\mathrm{e,cal}} - q_{\mathrm{e,exp}} \right\rvert_i$	(6)
Average relative error (ARE)	$\mathrm{ARE} = \frac{100}{n} \sum_{i=1}^{n} \left\lvert \frac{q_{\mathrm{e,cal}} - q_{\mathrm{e,exp}}}{q_{\mathrm{e,exp}}} \right\rvert_i$	(7)
Hyrbrid error function (HYBRID)	$\mathrm{HYBRID} = \frac{100}{n-p} \sum_{i=1}^{n} \left[\frac{(q_{\mathrm{e,cal}} - q_{\mathrm{e,exp}})^2}{q_{\mathrm{e,exp}}} \right]_i$	(8)
Marquardt's percent standard deviation (MPSD)	$\mathrm{MPSD} = 100 \sqrt{\frac{1}{n-p} \sum_{i=1}^{n} \left(\frac{q_{\mathrm{e,cal}} - q_{\mathrm{e,exp}}}{q_{\mathrm{e,exp}}} \right)_i^2}$	(9)
Chi-square	$\chi^2 = \sum \frac{(q_{\mathrm{e,exp}} - q_{\mathrm{e,cal}})^2}{q_{\mathrm{e,cal}}}$	(10)

for selecting the optimum isotherm parameters among them. This normalization procedure allows direct combination of these scaled errors and identifies the optimum parameters set by its minimum SNE values. The detailed calculation process was described by Foo, K.Y. and Kundu, S. [11,12]. Further, since the different error functions selected are presumed to cover a reasonably wide selection, it is plausible that the distribution of the experimental data does not give excessive weight either to high or low concentration ranges. In addition, in all of the five error methods it is assumed that both the liquid-phase concentration and the solid-phase concentration contribute equally to weighting the error criterion for the model solution procedure. Hence the difference in the solid phase concentration reflected the differences in the predicted concentrations for both phases.

The process of minimizing the respective error functions across the experimental concentration ranges examined yields the isotherm parameters. The isotherm parameters so obtained, together with the final SNE values, are presented in Table 4. The best fitted parameters for each isotherm model could be determined based on the minimum SNE values. The figures in bold type in Table 4 represent the optimum isotherm constants for Langmuir, Freundlich, Langmuir–Freundlich, and Toth isotherm obtained using the different error functions. The four isotherms are illustrated in Fig. 1. This figure shows the superposition of experimental results (points) and theoretical calculated points (lines). As shown in Table 4, the lowest SNE value is obtained using the ARE function for Langmuir isotherm, whereas the SAE method is effective for Freundlich isotherm. Isotherm parameters obtained using the SAE method would provide a better fit as the magnitude of the errors increased biasing the fit towards the high concentration data [13]. The HYBRID method provided the lowest SNE values for Langmuir–Freundlich and Toth isotherm, which are the three parameter models. This error function seems more adequate as it takes into account different numbers of the model parameters [13].

Though SNE values allow the comparison between error functions and the identification of the optimum isotherm constants for each isotherm model, it cannot identify the best fitted isotherm model [9]. To determine the best fitted isotherm model, χ^2 value of each isotherm model with the optimum parameters was calculated, which was shown in Table 4. On the basis of χ^2 values, the order of nonlinear best-fit was Langmuir–Freundlich model > Toth model > Freundlich model > Langmuir model. Consequently, the most suitable model for this sorption system was the Langmuir–Freundlich isotherm with q_{mLF} = 837.518 mg g^{-1}, K_{LF} = 10,369.509 M^{-1}, and m_{LF} = 0.578, while the Langmuir model seems not appropriate for the experimental results due to the significantly highest χ^2 value. This result indicates that the PAC used in the study is an energetically heterogeneous

Table 4
Isotherm constants with error analysis

Isotherm	SSE	SAE	ARE	HYBRID	MPSD
Langmuir					
q_{mL} (mg g^{-1})	337.943	340.132	**307.326**	302.593	254.229
K_L (M^{-1})	126782.225	126782.226	**173737.739**	173737.736	2733887.056
SNE	3.603	3.572	**3.415**	3.460	4.680
χ^2	–	–	**18.412**	–	–
Freundlich					
K_F (mg M$^{-1/nF}$ g^{-1})	34388.256	**46644.447**	46644.447	42556.332	46644.447
n_F	2.179	**2.056**	2.057	2.092	2.057
SNE	4.860	**3.981**	3.977	4.033	3.983
χ^2	–	**3.867**	–	–	–
Langmuir–Freundlich					
q_{mLF} (mg g^{-1})	580.271	837.518	1537.432	**837.518**	1537.432
K_{LF} (M^{-1})	29556.802	10369.509	2064.026	**10369.509**	2064.027
m_{LF}	0.650	0.572	0.527	**0.578**	0.528
SNE	4.674	4.102	4.196	**4.070**	4.222
χ^2	–	–	–	**2.583**	–
Toth					
q_{mT} (mg g^{-1})	1651.683	3178075.583	3178075.583	**5184.062**	3178075.583
K_T (μM^{-1})	258436.908	624969.302	624969.302	**258450.828**	624969.302
n_T	0.260	0.065	0.065	**0.181**	0.065
SNE	4.687	4.295	4.295	**4.282**	4.297
χ^2	–	–	–	**3.007**	3.197

Note: Values in bold represent minimum sum of normalized errors (SNE), Chi-square values (χ^2), and the corresponding isotherm parameters.

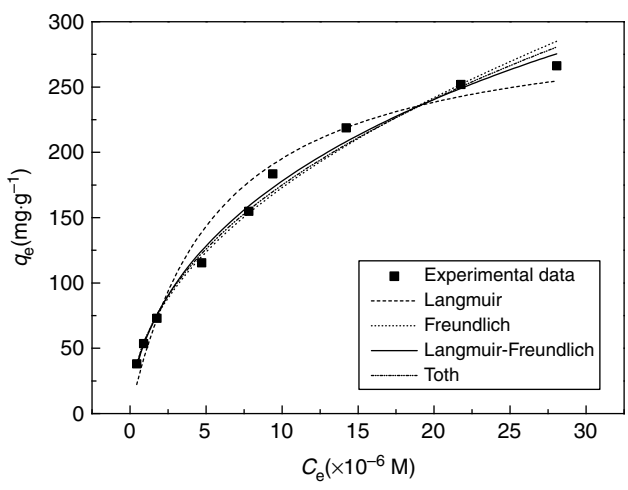

Fig. 1. Adsorption isotherm modeling of CB removal by PAC using nonlinear regression analysis (initial CB concentration = 3.7 mg l^{-1}, pH = 7.2 and temperature = 25 ± 0.3°C).

adsorbent, which is because the Langmuir–Freundlich isotherm assumes the adsorbent surface to be heterogeneous, as opposed to the Langmuir equation that assumes a homogeneous adsorbent.

3.2. Adsorption kinetics

The initial concentration of CB (C_0) and PAC dose (m_c) were considered to investigate the kinetics of CB adsorption onto PAC. The variation of q_t with time is shown in Fig. 2 at three different C_0, 2.07, 3.10, and 4.70 mg l^{-1} (Fig. 2(a)), and at three m_c, 32.3, 50, and 70 mg l^{-1} (Fig. 2(b)). The results obtained showed that q_t increases rapidly in the initial minutes, then increases with lower rate and finally reaches to the equilibrium. The data presented in Fig. 2(a) also show that the amount of CB adsorbed increases with increased C_0. It is manifested that the sorption increased for lower m_c at any specific time in Fig. 2(b).

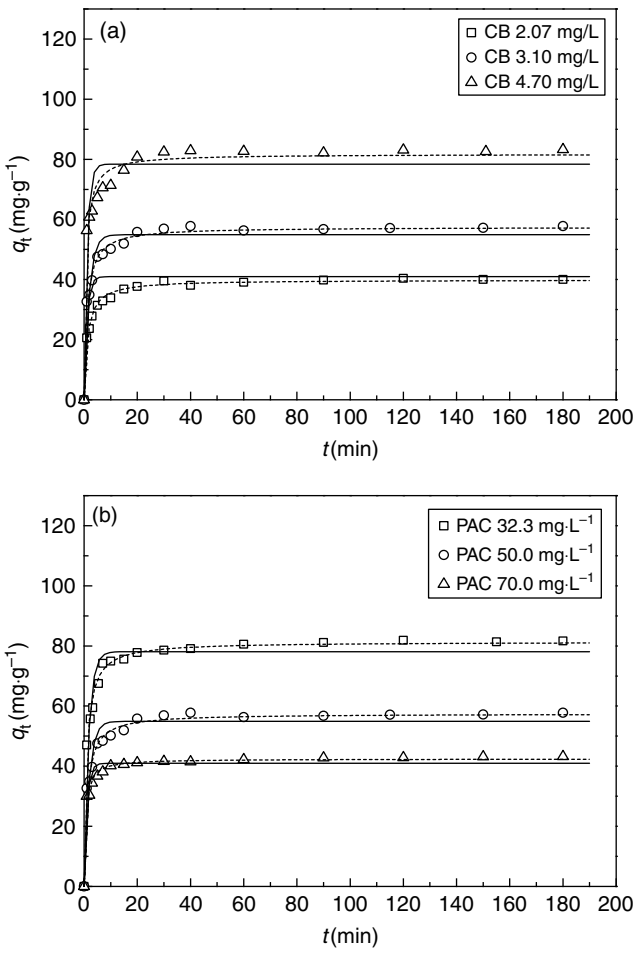

Fig. 2. Plot of sorbed capacity versus time at different initial concentrations of CB with PAC dose of 50 mg l^{-1} (a), and at different PAC doses with initial concentration of CB 3.10 mg l^{-1} (b) at temperature of 25°C, pH = 7.2. The symbols are experimental data, and the solid lines and dashed lines are calculated values by pseudo-first and pseudo-second order kinetic models, respectively.

Sorption kinetics, which describes the solute sorption rate, is an important characteristic in evaluating the efficiency of sorption. The adsorption kinetics of CB onto PAC was examined with different kinetic models.

3.2.1. Pseudo-first-order and pseudo-second-order kinetic models

Pseudo-first-order (Eq. 11) and pseudo-second-order (Eq. 12) models are the simplest and oldest kinetic models used to describe the adsorption kinetics [14,15]. The kinetic parameters involved in the two models for each case were estimated using the foregoing nonlinear regression analysis and Chi-square analysis. The calculated kinetic rate constants and their corresponding Chi-square value (χ^2) were given in Table 5. The solid lines and dashed lines in Fig. 2 represent the predicted kinetic isotherms by the obtained pseudo-first-order and pseudo-second-order models, respectively:

$$\ln(q_e - q_t) = \ln q_e - k_1 t \tag{11}$$

$$q_t = \frac{k_2 q_e^2 t}{1 + k_2 q_e t} \tag{12}$$

From the results in Table 5, the pseudo-second-order equation was the model that gave a better fit to the experimental data, because its Chi-square values (χ^2) are lower than 2.560, while those for pseudo-first-order model are $2.958 \le \chi^2 \le 8.587$. Although the Chi-square values (χ^2) are lower for pseudo-second-order model, there is a deviation from this model for short times (when t is less than 20 min) at all cases in Fig. 2 (dashed lines).

As shown in Table 5, the values of rate constants (k_1 and k_2), are found to increase with increasing C_0 and m_c,

Table 5
The obtained constants of pseudo-first-order and pseudo-second-order kinetic models with Chi-square values (χ^2), at different initial concentrations of CB (C_0) with PAC dose of 50 mg l^{-1} and at different PAC doses (m_c) with initial concentration of CB 3.10 mg l^{-1}

Parameters	Pseudo-first-order model			Pseudo-second-order model		
	q_e (mg g^{-1})	k_1 (min^{-1})	χ^2	q_e (mg g^{-1})	k_2 (g mg^{-1} min^{-1})	χ^2
C_0 (mg l^{-1})						
2.07	38.085	0.487	3.566	39.903	0.020	0.613
3.10	54.925	0.537	5.478	57.469	0.016	1.374
4.70	78.346	0.882	8.587	81.743	0.018	2.560
m_c (mg l^{-1})						
32.3	78.078	0.528	6.015	81.374	0.013	1.050
50	54.925	0.537	5.478	57.469	0.016	1.374
70	40.950	0.912	2.958	42.433	0.041	0.685

except for the values of rate constant (k_2) at different C_0. This result indicates that the main disadvantage of both pseudo-first-order and pseudo-second-order models is the dependency of their rate constants (k_1 and k_2) to the initial concentration of solute and the dose of adsorbent. Therefore the rate constants (k_1 and k_2) are really pseudo-constants. This dependency has been shown both experimentally [16,17] and theoretically [18].

3.2.2. Langmuir–Freundlich kinetic model

A favorite model for analysis of adsorption kinetics is Eq. (13) which is also called Langmuir–Freundlich kinetic model [19]:

$$\frac{d\theta_t}{dt} = k_a C_t (1-\theta_t)^{1/m_{LF}} - k_d \theta_t^{1/m_{LF}} \tag{13}$$

where $\theta_t = q_t/q_{mLF}$ is the surface fractional coverage of adsorbate at time t, and k_a (M^{-1} min^{-1}) and k_d (min^{-1}) are the adsorption and desorption rate constants, respectively.

This model shows that simultaneous studies of adsorption equilibrium are essential for a good understanding of adsorption kinetics. Generally, C_t in Eq. (13) is not constant and decreases with increasing the amount of adsorption (θ_t) during adsorption process as:

$$C_t = C_0 - \frac{m_c q_{mLF}}{10^6 M_W}\theta_t \tag{14}$$

where q_{mLF} is the Langmuir–Freundlich maximum adsorption capacity (mg g^{-1}), M_W is the molecular weight of adsorbate (g mol^{-1}). So by substitution of Eq. (14) into Eq. (13) we have:

$$\frac{d\theta_t}{dt} = k_a\left(C_0 - \frac{m_c q_{mLF}}{10^6 M_W}\theta_t\right)(1-\theta_t)^{1/m_{LF}} - k_d \theta_t^{1/m_{LF}} \tag{15}$$

One of the advantages of Eq. (15) is that the rate of adsorption and desorption can be separated. Based on Eq. (15), the rates of adsorption (r_a, min^{-1}) and desorption (r_d, min^{-1}) can be written as:

$$r_a = k_a\left(C_0 - \frac{m_c q_{mLF}}{10^6 M_W}\theta_t\right)(1-\theta_t)^{1/m_{LF}} \tag{16}$$

$$r_d = k_d \theta_t^{1/m_{LF}} \tag{17}$$

On the basis of extended geometric method proposed by Azizian etc. [20] for Eq. (15), the rate constant of adsorption (k_a) can be computed by:

$$k_a \approx \frac{k_0}{C_0\left(1-\frac{t_L}{2t_e}\right) - k_0 t_L \frac{m_c q_{mLF}}{10^6 M_W}\left(\frac{1}{2} - \frac{1}{3m_{LF}}k_0 t_L + \frac{(1-m_{LF})}{8{m_{LF}}^2}k_0^2 t_L^2\right)} \tag{18}$$

where k_0 is the initial slope of θ_t vs. t plot (linear region), t_L the initial time of adsorption where θ_t vs. t is linear, t_e the equilibrium time. q_{mLF} and m_{LF} can be easily found from the Langmuir–Freundlich adsorption isotherm. So the input data of Eq. (18) can be easily obtained from the experimental data of θ_t vs. t and also adsorption isotherm. Desorption rate constant (k_d in Eq. (15)) can be easily computed by:

$$k_d = \frac{k_a}{K_{LF}} \tag{19}$$

where K_{LF} is the Langmuir–Freundlich equilibrium constant.

Equilibrium studies on the adsorption of CB onto PAC showed that the present system obeys Langmuir–Freundlich isotherm with q_{mLF} = 837.518 mg g^{-1}, K_{LF} = 10,369.509 M^{-1}, and m_{LF} = 0.578. Analysis of kinetic experimental data showed that θ_t increases with time as a linear form up to 5 min and reaches equilibrium at 180 min, in all cases shown in Fig. 3. Thus the time of 5 min and 180 min was selected as t_L and t_e, respectively. The initial slopes of θ_t vs. t (i.e., k_0) were calculated for different C_0 and m_c were listed in Table 5, respectively. These values show that k_0 is a function of C_0 and m_c. The values of k_0 increase with increasing C_0 but decreasing m_c. By using the above parameters, the values of adsorption and desorption rate constants (k_a and k_d) can be calculated by Eqs. (18) and (19), respectively. The values of calculated rate constants (k_a and k_d) at different C_0 and m_c are listed in Table 6. The values of k_a at different C_0 and m_c are in the same range and their small differences are due to experimental random error. Similar character was observed in the values of k_d at different C_0 and m_c. These results show that extended geometric method can evaluate the rate constant (initial adsorbate concentration and adsorbent dose independent) of adsorption of Langmuir–Freundlich kinetic with a good accuracy. The average value of k_a is 951.776 M^{-1} min^{-1}. By using of equilibrium constant (K_{LF} = 10,369.509 M^{-1} min^{-1}) and average value of k_a, the average value of desorption rate constant (k_d) is 0.0918 min^{-1} calculated by Eq. (19).

The rates of adsorption and desorption were calculated by Eqs. (16) and (17) using the rate constants obtained by extended geometric method. The variation of calculated r_a and r_d with time at C_0 = 3.10 mg l^{-1} M and PAC dosage of 50 mg l^{-1} is shown in Fig. 4. This

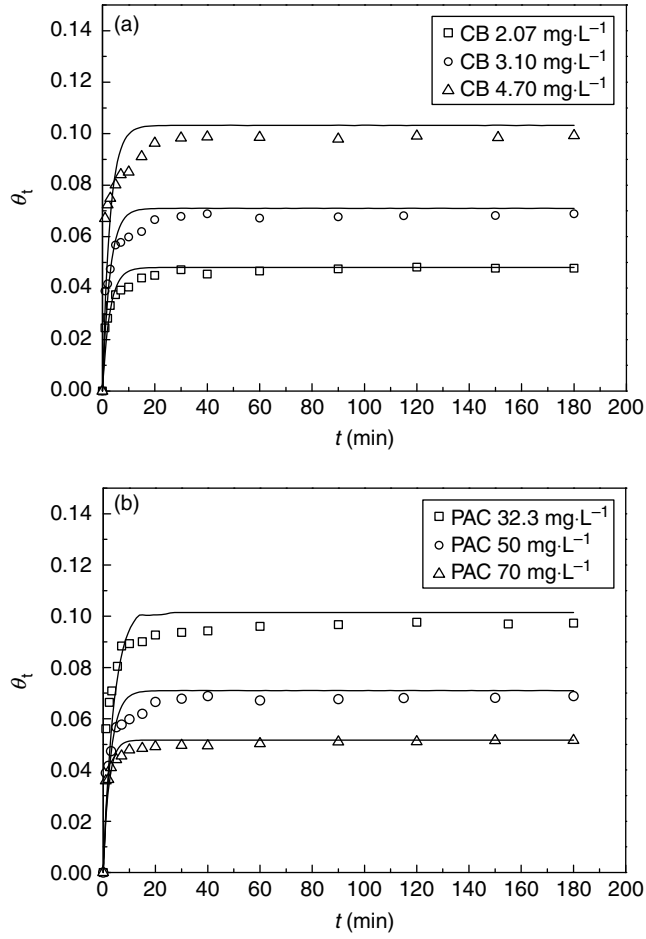

Fig. 3. Variation of θ_t with time at different initial concentrations of CB with PAC doses of 50 mg l^{-1} (a), and at different PAC doses with initial concentration of CB 3.10 mg l^{-1}. The symbols are experimental data and solid lines are calculated values by Eq. (15).

Table 6
The kinetics parameters of CB adsorption onto PAC at different initial concentration of CB (C_0) with PAC dose of 50 mg l^{-1} and at different PAC doses (m_c) with initial CB concentration of 3.10 mg l^{-1} at 25°C

Parameters	k_0 (min^{-1})	k_a (M^{-1} min^{-1})	k_d (min^{-1})
C_0 (mg l^{-1})			
2.07	9.430×10^{-3}	950.843	0.0917
3.10	1.424×10^{-2}	950.548	0.0917
4.70	2.147×10^{-2}	951.850	0.0918
m_c (mg l^{-1})			
32.3	1.705×10^{-2}	952.606	0.0919
50	1.424×10^{-2}	950.548	0.0917
70	1.201×10^{-2}	954.258	0.0920

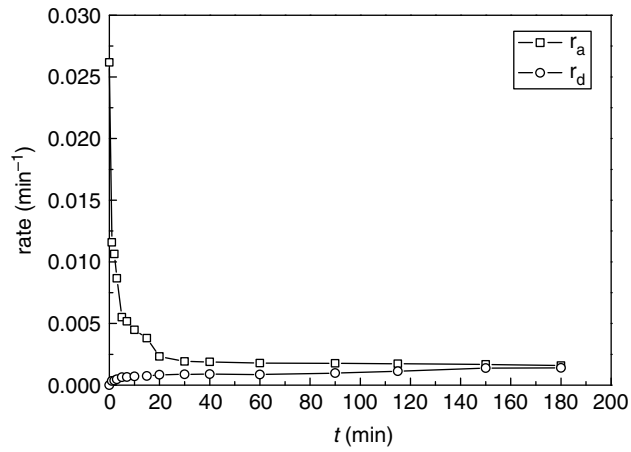

Fig. 4. Calculated rates of adsorption and desorption of CB onto PAC (25°C, CB concentration 3.10 mg l^{-1}, PAC dosage of 50 mg l^{-1}).

figure shows that the rate of adsorption of CB onto PAC is higher than its rate of desorption at short initial times, and the adsorption system is close to equilibrium at long times. The low values of r_d indicate that the adsorbed CB remains almost stable on the PAC.

It is necessary to compare the calculated and experimental values of θ_t at various times to examine the validity of extended geometric method. By using of the average values of k_a and k_d from extended geometric method, Eq. (15) was numerically calculated with the MATLAB ode solver (ode45). The numerical results for the variation of θ_t with time were obtained and were shown as solid lines in Fig. 3 for different C_0 and m_c. A good agreement between the experimental data and the results of Eq. (15) is observed for the lower C_0 and the higher m_c (Fig. 3). However, the calculated and experimental values did not match completely for higher C_0 and lower m_c at time more than 10 min, when the most significant deviations can be seen. These deviations may be due to (1) three approximations in extended geometric method, (2) the use of the average value of k_a and k_d for all C_0 and m_c, (3) experimental errors and (4) adsorbate–adsorbate interactions that may are important at high loading (or high concentrations) which did not considered in Langmuir–Freundlich model.

It is interesting to note that one just needs initial kinetic data at one initial adsorbate concentration and one adsorbent dosage to estimate rate constants with extended geometric method. Also by using the Langmuir–Freundlich kinetic model and calculated rate constants, it is possible to predict the variation of θ_t with time in the whole region: from short initial times to long times when the system is close to equilibrium for different C_0 and m_c.

4. Conclusions

The adsorption of CB from aqueous solution by a wood-based PAC was evaluated in this study. The conclusions are as follows:

1. Langmuir–Freundlich isotherm model was the best-fitting model for CB adsorption onto PAC in aqueous solution, and the maximum adsorption capacity was 837.518 mg g^{-1}.
2. The rate constants of the pseudo-fist-order and pseudo-second-order kinetic models are dependent on the initial CB concentration and PAC dose.
3. The rate constants of Langmuir–Freundlich kinetic model obtained by extended geometric method are independent of initial concentration of CB and PAC dose. The rate constants can be applied at any initial concentration of CB and PAC dose, and therefore are useful for process design.
4. The results show that PAC is a stable and effective adsorbent for removal of CB from solution in water treatment.

Acknowledgments

The authors gratefully acknowledge financial support from the National High Technology Research and Development Program of China (Grant No. 2008AA06A414), National Natural Science Foundation of China (Project 50808134 and 51178322), and International Science & Technology Cooperation Program of China (Project 2010DFA92090).

Symbols

C_e — the equilibrium solute concentration (M)
C_0 — the initial concentration of chlorobenzene (M)
C_t — the concentration of solute at time t (M)
m_c — the dose of PAC (mg l^{-1})
q_e — the amount of adsorbate adsorbed at equilibrium (mg g^{-1})
q_t — the amount of adsorbate adsorbed at time t (mg g^{-1})
q_{mL} — the Langmuir maximum adsorption capacity (mg g^{-1})
q_{mLF} — the Langmuir–Freundlich maximum adsorption capacity (mg g^{-1})
q_{mT} — the Toth maximum adsorption capacity (mg g^{-1})
K_L — the Langmuir adsorption equilibrium constant (M^{-1})
K_F — the Freundlich isotherm equilibrium constant (mg $M^{-1/nF}$ g^{-1})
K_{LF} — the Langmuir–Freundlich isotherm equilibrium constant (M^{-1})
K_T — the Toth isotherm equilibrium constant (M^{-1})
n_F — the Freundlich constant indicative of the intensity of the adsorption
m_{LF} — the Langmuir–Freundlich model exponent
n_T — the Toth model exponent
χ^2 — Chi-square value
$q_{e,cal}$ — the amount of adsorbate adsorbed at equilibrium, calculated value, mg g^{-1}
$q_{e,exp}$ — the amount of adsorbate adsorbed at equilibrium, experimental value, mg g^{-1}
θ_t — the surface fractional coverage of adsorbate at time t
M_W — the molecular weight of adsorbate (g mol^{-1})
k_1 — the pseudo-first-order sorption rate coefficient (min^{-1})
k_2 — the pseudo-second-order rate coefficient (g mg^{-1} min^{-1})
k_0 — the initial slope of θ_t vs. t plot (linear region), min^{-1}
k_a — the adsorption rate constant (M^{-1} min^{-1})
k_d — the desorption rate constant (min^{-1})
r_a — the rate of adsorption (min^{-1})
r_d — the rate of desorption (min^{-1})

References

[1] X.-K. Zhao, G.-P. Yang, P. Wu and N.-H. Li, Study on adsorption of chlorobenzene on marine sediment, J. Colloid Interface Sci., 243 (2001) 273–279.
[2] R. Feltens, I. Mögel, C. Röder-Stolinski, J.-C. Simon, G. Herberth and I. Lehmann, Chlorobenzene induces oxidative stress in human lung epithelial cells in vitro, Toxicol. Appl. Pharmacol., 242 (2010) 100–108.
[3] W. Peirano, Health assessment document for chlorinated benzenes. Final Report, in, U.S. Environmental Protection Agency, Washington, D.C., 1985.
[4] R.R. Bansode, J.N. Losso, W.E. Marshall, R.M. Rao and R.J. Portier, Adsorption of volatile organic compounds by pecan shell- and almond shell-based granular activated carbons, Bioresour. Technol., 90 (2003) 175–184.
[5] D.R.U. Knappe, Y. Matsui, V.L. Snoeyink, P. Roche, M.J. Prados and M.-M. Bourbigot, Predicting the capacity of powdered activated carbon for trace organic compounds in natural waters, Environ. Sci. Technol., 32 (1998) 1694–1698.
[6] R. Sennour, G. Mimane, A. Benghalem and S. Taleb, Removal of the persistent pollutant chlorobenzene by adsorption onto activated montmorillonite, Appl. Clay Sci., 43 (2009) 503–506.
[7] Y. Shu, L. Li, Q. Zhang and H. Wu, Equilibrium, kinetics and thermodynamic studies for sorption of chlorobenzenes on CTMAB modified bentonite and kaolinite, J. Hazard. Mater., 173 (2010) 47–53.
[8] S.J.R.a.V.L. Snoeyink, Evaluating GAC adsorption capacity, J. Am. Water Works Assoc., 75 (1983) 406–413.
[9] F. Gimbert, N. Morin-Crini, F. Renault, P.-M. Badot and G. Crini, Adsorption isotherm models for dye removal by cationized starch-based material in a single component system: Error analysis, J. Hazard. Mater., 157 (2008) 34–46.
[10] M.C. Ncibi, Applicability of some statistical tools to predict optimum adsorption isotherm after linear and non-linear regression analysis, J. Hazard. Mater., 153 (2008) 207–212.
[11] K.Y. Foo and B.H. Hameed, Insights into the modeling of adsorption isotherm systems, Chem. Eng. J., 156 (2010) 2–10.

[12] S. Kundu and A.K. Gupta, Arsenic adsorption onto iron oxide-coated cement (IOCC): regression analysis of equilibrium data with several isotherm models and their optimization, Chem. Eng. J., 122 (2006) 93–106.
[13] S.J. Allen, G. McKay and J.F. Porter, Adsorption isotherm models for basic dye adsorption by peat in single and binary component systems, J. Colloid Interface Sci., 280 (2004) 322–333.
[14] S. Lagergren, Kungliga svenska vetenkapsademiens, Handlingar, 24 (1898) 1–39.
[15] G. Blanchard, M. Maunaye and G. Martin, Removal of heavy metals from waters by means of natural zeolites, Water Res., 18 (1984) 1501–1507.
[16] S. Azizian and B. Yahyaei, Adsorption of 18-crown-6 from aqueous solution on granular activated carbon: a kinetic modeling study, J. Colloid Interface Sci., 299 (2006) 112–115.
[17] F. Al Mardini and B. Legube, Effect of the adsorbate (Bromacil) equilibrium concentration in water on its adsorption on powdered activated carbon. Part 2: kinetic parameters, J. Hazard. Mat., 170 (2009) 754–762.
[18] S. Azizian, Kinetic models of sorption: a theoretical analysis, J. Colloid Interface Sci., 276 (2004) 47–52.
[19] C.W. Cheung, J.F. Porter and G. McKay, Sorption kinetics for the removal of copper and zinc from effluents using bone char, Sep. Purif. Technol., 19 (2000) 55–64.
[20] S. Azizian, M. Haerifar and J. Basiri-Parsa, Extended geometric method: a simple approach to derive adsorption rate constants of Langmuir–Freundlich kinetics, Chemosphere, 68 (2007) 2040–2046.